

## SEDIMENT PROCESSES AND MANGROVE-HABITAT EXPANSION ON A RAPIDLY-PROGRADING MUDDY COAST, NEW ZEALAND

Andrew Swales<sup>1</sup>, Samuel J. Bentley<sup>2</sup>, Catherine Lovelock<sup>3</sup>, Robert G. Bell<sup>1</sup>

1. NIWA, National Institute of Water and Atmospheric Research, P.O. Box 11-115 Hamilton, New Zealand. [a.swales@niwa.co.nz](mailto:a.swales@niwa.co.nz), [r.bell@niwa.co.nz](mailto:r.bell@niwa.co.nz)
2. Earth-Sciences Department, 6010 Alexander Murray Building, Memorial University of Newfoundland, St John's NL, Canada A1B 3X5. [sjb@esd.mun.ca](mailto:sjb@esd.mun.ca)
3. Centre for Marine Studies, University of Queensland, St Lucia, Queensland, QLD 4072, Australia. [C.lovelock@uq.edu.au](mailto:C.lovelock@uq.edu.au)

**Abstract:** Mangrove-habitat expansion has occurred rapidly over the last 50 years in the 800 km<sup>2</sup> Firth-of-Thames estuary (New Zealand). Mangrove forest now extends 1-km seaward of the 1952 shoreline. The geomorphic development of this muddy coast was reconstructed using dated cores (<sup>210</sup>Pb, <sup>137</sup>Cs, <sup>7</sup>Be), historical-aerial photographs and field observations to explore the interaction between sediment processes and mangrove ecology. Catchment deforestation (1850s–1920s) delivered millions of m<sup>3</sup> of mud to the Firth, with the intertidal flats accreting at 20 mm yr<sup>-1</sup> before mangrove colonization began (mid-1950s) and sedimentation rates increased to ≤ 100 mm yr<sup>-1</sup>. <sup>210</sup>Pb data show that the mangrove forest is a major long-term sink for mud. Seedling recruitment on the mudflat is controlled by wave-driven erosion. Mangrove-habitat expansion has occurred episodically and likely coincides with calm weather. The fate of this mangrove ecosystem will depend on vertical accretion at a rate equal to or exceeding sea level rise.

### INTRODUCTION

Enhanced sedimentation is occurring globally in estuaries due to increased catchment sediment yields associated with land-use changes (e.g., Thrush et al., 2004) particularly in the small and mountainous catchments that characterise the active-tectonic margins of the Pacific Rim (Milliman and Syvitski, 1992). Increased soil erosion has accelerated the infilling of estuaries, which have become progressively intertidal. In many temperate and tropical settings these intertidal flats have been colonized by mangroves (Neil, 1998; Ellis et al., 2004). Once established, mangroves influence estuarine sedimentary processes and long-term geomorphic evolution (Thom et al., 1975). Mangroves enhance mud accumulation by dampening currents and attenuating waves so that sediment accumulation rates (SAR) are highest within the fringes of mangrove forests, and decline with distance from the mangrove fringe (Furukawa et al., 1997). While mangroves may

stabilize sediments, provide fish nurseries and enhance water quality, mangrove-habitat expansion is not always desirable. In estuaries that previously had sandy substrates mangrove colonization and/or habitat expansion enhances long-term mud accumulation.

This major change in substrate type from sand to mud, results in loss of biodiversity and changes in benthic community structure (Ellis et al., 2004).

In New Zealand (N.Z.), the grey mangrove (*Avicennia marina*), which is a frost-sensitive species, occurs in North Island estuaries above 38°S latitude and can colonize intertidal flats down to mean sea level (MSL), where seedlings are submerged for  $\leq 6$  hr per tide (Clarke and Myerscough, 1993). Mangrove-habitat expansion has occurred in many estuaries within their range in recent decades (Burns and Ogden 1985; Ellis et al., 2004) as has also occurred for introduced-invasive species such as the Cordgrass, *Spartina anglica*, (Swales et al., 2004). This process has been exacerbated by estuary infilling, forming extensive intertidal flats potentially suitable for colonization. This natural infilling process has accelerated over the last 150 years as sediment loads have increased due to catchment deforestation and SAR of  $< 0.5 \text{ mm yr}^{-1}$  before deforestation have increased by an order of magnitude (Hume and McGlone, 1986, Swales et al., 2002). However, mangrove-habitat expansion observed over the last 50 years has occurred decades after catchment deforestation. Alternative explanations for this relatively recent expansion include climate change and increasing nutrient inputs associated with agricultural activities.

Mangrove-habitat expansion has been particularly rapid in the Firth of Thames, which is a 800 km<sup>2</sup> meso-tidal estuarine embayment on the east-coast of the North Island (37°S 175.4°E) 70-km south-east of Auckland (Fig. 1). Captain James Cook visited the Firth in 1769 and noted the presence of mangrove along the lower Waihou river (Brownell, 2004).

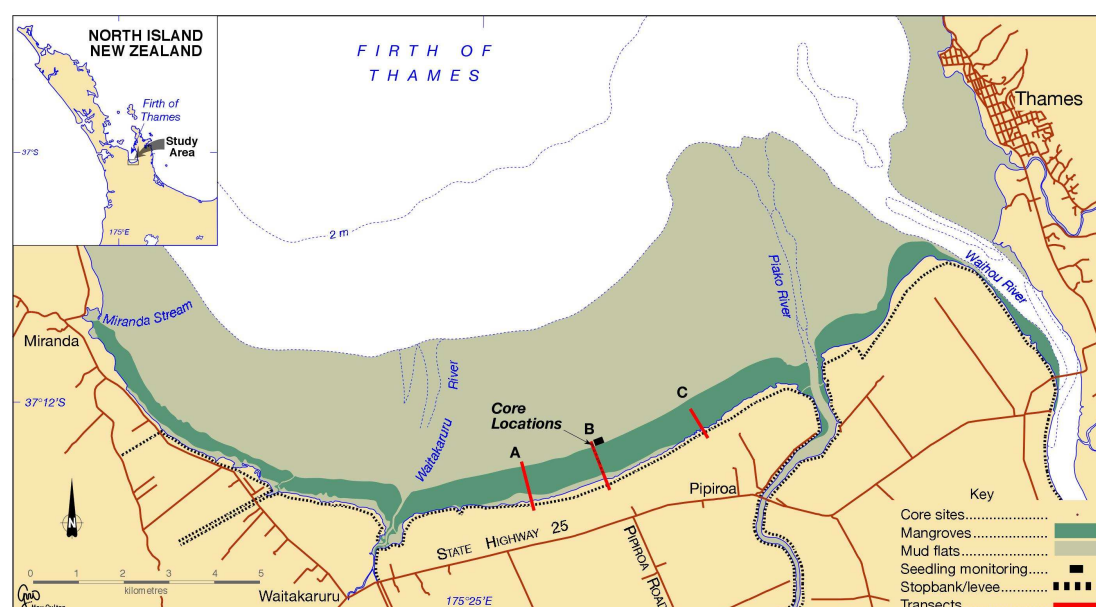


**Fig. 1.** Location of the study area, southern Firth of Thames, New Zealand.

Aerial photographs show that mangrove-habitat was restricted to delta deposits at river mouths as recently as the early 1950's. Today, mangrove habitat in the southern Firth extends 1-km seaward of the 1952 shoreline and covers 11 km<sup>2</sup> of former intertidal mudflat. The seabed elevation is now 0.1–0.2 m above mean high-water spring (MHWS) tide level so that the mangrove forest is only infrequently inundated.

This rapid mangrove-habitat expansion raises a number of questions that are relevant to the fate of mangrove systems and estuaries: what has triggered mangrove-habitat expansion decades after deforestation; how are mangroves altering estuaries; how does seedling recruitment occur on wave-exposed mudflats; and what is the long-term fate of these mangrove systems given the potential effects of climate change? In this paper we reconstruct the recent geomorphic development of this muddy coast and consider the interaction between sediment processes, geomorphology and mangrove ecology.

## **STUDY SITE**

The Firth of Thames estuarine embayment occupies the Hauraki Depression, which is a structural graben (Healy, 2002) bounded to the east and west by the Coromandel and Hunua Ranges respectively. To the south are the low-lying Hauraki Plains, which are underlain by estuarine sediments (Woodroffe et al., 1983). The Firth receives runoff from a 3600 km<sup>2</sup> catchment and primarily from the Waihou (1966 km<sup>2</sup>) and Piako (1476 km<sup>2</sup>) Rivers, which deliver an estimated 150,000 t yr<sup>-1</sup> and 35,000 t yr<sup>-1</sup> of suspended sediment respectively. The Waihou River has delivered sediment to the Firth for the last 20,000 years. Shoreline-progradation rates have averaged 1.7 m yr<sup>-1</sup> over the last 6,500 years (Brownell, 2004) and a chenier plain has formed in the last 3,600 years along the western shore of the Firth (Woodroffe et al., 1983).

## **History**

Pre-human catchment landcover consisted of podocarp–hardwood forests on the steepplands while the Hauraki Plains were occupied by freshwater marshes and swamp forests of the podocarp Kahikatea. Maori arrived about 1,000 years ago and forest clearance was restricted to the rivers banks. European settlers arrived in the mid-1800s and large-scale deforestation began shortly after in the Coromandel ranges associated with logging and gold-mining activities (Brownell, 2004). These activities substantially increased sediment loads to the Firth. Hydrographic surveys conducted by the Public Works Department in 1882 and 1918 indicate that *c.* 6.9 x 10<sup>6</sup> m<sup>3</sup> of sediment was deposited within a 16 km<sup>2</sup> area of the lower Waihou River and its tidal delta (Fig. 1) and an estimated 36.7 x 10<sup>6</sup> m<sup>3</sup> was deposited in the 210 km<sup>2</sup> southern Firth. Development of the Hauraki Plains was delayed until drainage works began in 1905 with a stop-bank/levee constructed along the southern shore of the Firth and the tidal reaches of the rivers. By 1920 some 162 km<sup>2</sup> of swamp had been converted to pasture (Brownell, 2004). The 1932 storm flooded the entire Hauraki Plains and consequently the heights of stop-banks were increased. These engineering works constrained floodwaters to the river channels and are likely to have increased sediment delivery to the Firth.

## **Estuary characteristics**

The Firth shoals from a maximum depth of 35 m at its inlet. Tides are semi-diurnal, with average spring- and neap-tidal ranges of 2.8-m and 2-m respectively. Tidal-current speeds are typically  $\leq 0.2 \text{ m s}^{-1}$  on the intertidal flats. Estuarine circulation and residual-tidal currents trap river-borne suspended sediments within the Firth (Healy, 2002). Northerly winds generate short-period ( $T < 6 \text{ s}$ ) waves typically  $< 1 \text{ m}$  high (Woodroffe et al., 1983). The historical rate of sea level rise at Auckland (1904–1999) has averaged  $1.3 \text{ mm yr}^{-1}$ . The large tidal range, shallow bed slope ( $0.03^\circ$ ) and fine-sediment supply has built some  $70 \text{ km}^2$  of intertidal-mudflats along the southern shore of the Firth (Fig. 1). Mudflat morphology is similar to that described for the muddy coast of Surinam, South America (Augustinus, 1980; Wells and Colman, 1981). The lower-intertidal flat is characterized by fluid mud, while a “mud bastion” morphology of isolated consolidated-mud mounds  $\leq 20\text{-cm}$  high develops on the middle–upper intertidal flat above  $0.7 \text{ m MSL}$ . On the Surinam coast, these features have been interpreted as remnants of an eroded mudflat (Augustinus, 1980, Fig. 7). Above  $0.8 \text{ m MSL}$ , the mud bastions are replaced by a  $300\text{-m}$  wide band of large-scale “mud forms” that resemble an irregular ridge-runnel system. These shore-normal, often bifurcating ridges, are  $\leq 0.25 \text{ m}$  high with wavelengths  $\leq 2 \text{ m}$  and sinuous crests up to  $50 \text{ m}$  long. These features are not drainage channels as the runnels are isolated from each other. This intertidal morphology is characteristic of a mesotidal, moderately wave-exposed, muddy coast, with large mud supply, high suspended sediment concentrations (SSC) and rapid sedimentation. In similar muddy-coast environments, near-bed SSC in the range  $10^3\text{--}10^4 \text{ mg l}^{-1}$  increase fluid density sufficiently to attenuate shoaling waves (Wells and Coleman, 1981; Mehta, 2002).

## **METHODS**

### **Mangrove-habitat mapping, forest structure and pore-water salinity**

Mangrove-habitat expansion was mapped from vertical aerial photographs of the southern Firth taken between 1952 and 2002. The digitized photographs were geo-referenced and analyzed using ARC-GIS software. Mangrove-forest structure was characterized at *c.*  $20\text{-m}$  intervals across-shore using the point-center-quarter method (Cintrón and Schaffer-Novelli, 1984). Pore-water salinity at  $30\text{-cm}$  depth was measured using the methods of McKee et al. (1988). A relationship between pore water salinity and forest height was tested using regression analysis.

### **Intertidal-flat elevation and tides**

Intertidal-flat elevations were measured along three transects (A–C) at *c.*  $2\text{-km}$  intervals alongshore and up to  $1200\text{-m}$  seaward of the stop-bank/levee (Fig. 1) to determine the large-scale shore morphology and relate the sediment-cores to the mean sea level (MSL) datum. Elevations were measured to  $\pm 0.5 \text{ cm}$  using a Geodimeter Model 464 total station. A sea-level record (1992–present) from Tararu ( $3 \text{ km}$  north of Thames, Fig. 1) was analyzed to determine: (1) the duration of tidal inundation (2004–2006) of the mangrove forest; and (2) exceedance probability (%) for predicted high-tide levels (1900–1999 AD). The inundation time for specified vertical levels was determined for predicted tides (using tidal constituents for 2004–2006); and the measured (storm) tides.

### Sediment cores

Replicate sediment cores 7.5-cm-diameter and  $\leq 1.9$ -m long were collected from the mangrove forest along Transect B (February 2005) using a piston corer (Fig. 1, **LC sites** 3–11). A 0.7-m-long push core (site LC-12) was also 50-m seaward of the mangrove seaward edge of vegetation (SEV). Cores were also collected from the mudflats (**T sites**, Feb. 2006) up to 1-km seaward of the mangrove SEV using open-ended, three-sided Perspex trays (0.7 m deep, 2.5 x 19 cm). The trays were pushed into the sediment and then the fourth side inserted to minimize fabric distortion. Core names (e.g., T-50) indicate the seaward distance (m) of the site from the mangrove SEV. Core-compression was  $< 5\%$  in all cases. The LC cores were logged and sub-sampled at intervals in 2-cm-thick slices for radioisotope, bulk density and particle-size analysis. Particle-size was determined using an Ankersmid CIS-100 “time-of-transition” (TOT) stream-scanning-laser particle sizer. Sediment samples were wet-sieved through a 2-mm sieve to remove vegetation fragments and shell hash and dispersed in an ultra-sonic bath for 10 minutes before and during analysis. Sediment fabric was determined from x-radiographs prior to sub-sampling. The cores were sectioned into 2-cm-thick longitudinal slabs and imaged using a Phillips Model Macrotank 205 X-ray generator with Kodak AA400 film (50 kV, 5 mA, 1.1 min) and digitized using a Nikon D1x digital SLR camera (ISO 125, TIFF). X-radiographs of the T-site cores were obtained using a Thales Flash-scan 35 digital X-ray panel detector, illuminated by a Kramex PX15HF portable X-ray generator (60 kV, 15mA, 3 s). After imaging, these cores were sub-sampled at 1–2 cm intervals for analysis of beryllium-7 ( $^7\text{Be}$ , half life,  $t_{1/2}$  53 days) by gamma spectrometry.

SAR were estimated from lead-210 ( $^{210}\text{Pb}$ ,  $t_{1/2}$  22.3 yr) and caesium-137 ( $^{137}\text{Cs}$ ,  $t_{1/2}$  30 yr). The cosmogenic radioisotope  $^7\text{Be}$  is particle reactive and tends to be concentrated in aquatic systems, making it a useful sediment tracer in fluvial-marine systems at seasonal timescales. Radioisotope concentrations expressed in S.I. units of Becquerel (disintegration  $\text{s}^{-1}$ ) per kilogram ( $\text{Bq kg}^{-1}$ ) were determined by gamma-spectrometry. Dry samples (50–60 g) were counted for 23 hrs using a Canberra Model BE5030 hyper-pure germanium detector. The unsupported or excess  $^{210}\text{Pb}$  concentration ( $^{210}\text{Pb}_{\text{ex}}$ ) was determined from the  $^{226}\text{Ra}$  ( $t_{1/2}$  1622 yr) assay after a 30-day ingrowth period for  $^{222}\text{Rn}$  ( $t_{1/2}$  3.8 days) gas in samples embedded in epoxy resin. Gamma spectra of  $^{226}\text{Ra}$ ,  $^{210}\text{Pb}$  and  $^{137}\text{Cs}$  were analysed using Genie2000 software.  $^7\text{Be}$  concentrations in the T-core sediments were also obtained by gamma spectrometry, with 10-g dry samples sealed in petri dishes counted for 24 h. The  $^{210}\text{Pb}_{\text{ex}}$  profiles in each core were used to determine: (1) time-averaged SAR from regression analysis of natural log-transformed data; (2)  $^{210}\text{Pb}_{\text{ex}}$  inventory ( $A$ ,  $\text{Bq cm}^{-2}$ ) and; (3) mean annual supply rate ( $P$ ,  $\text{Bq cm}^{-2} \text{ yr}^{-1}$ ) based on the  $^{210}\text{Pb}$  decay co-efficient ( $k$ ,  $0.0311 \text{ yr}^{-1}$ ). These data were compared with the  $^{210}\text{Pb}$  atmospheric flux ( $0.006 \text{ Bq cm}^{-2} \text{ yr}^{-1}$ ) measured at Auckland. SAR were estimated from  $^{137}\text{Cs}$  profiles based on the maximum depth of  $^{137}\text{Cs}$  in each core and included corrections for sediment mixing indicated by  $^7\text{Be}$  profiles. In NZ,  $^{137}\text{Cs}$  deposition from the atmosphere was first detected in 1953 (Swales et al., 2002).

### Propagule and seedling establishment and recruitment

The establishment and survival of recently-settled propagules and seedlings on the wave-exposed mudflat was monitored over a 180-day period from January 2006 in an area immediately east of Transect B (Fig. 1). Three replicate sites *c.* 100-m apart alongshore were monitored each with ten 0.16 m<sup>2</sup> quadrats located on the top of the mud forms at 20 m, 70m and 120 m from the mangrove SEV. Propagule and seedlings numbers and their developmental stage (i.e., # of leaf pairs) were recorded and measurements repeated after 23, 44, 60 and 180 days. Data were pooled for each site by proximity grouping and cumulative survivorship was calculated as the proportion of propagules or seedlings remaining. Survivorship data were log transformed and analysed by repeated measures ANOVA where either site or proximity to the mangrove were fixed effects in the model.

## RESULTS

### Mangrove-habitat expansion

Historical-aerial photographs show that mangroves colonized the mudflat close to LC-3 between 1952 and 1963 and some 300-m seaward of the 1952 shoreline (Fig. 2a) and by 1963 had formed a 50-m wide stand. Subsequently, the mangrove forest spread seaward and, to a more limited extent, landward. By 1977 the mangrove SEV was located near LC-6 and by 1987 the SEV had extended to LC-8, some 726-m from the 1952 shoreline. By 2002 the mangrove-forest distribution was similar to that we surveyed in 2005.

### Large-scale mudflat morphology and tides

The shore profile has a convex-upward shape (Fig. 2a) that is characteristic of stable or prograding muddy-coasts (Mehta, 2002).

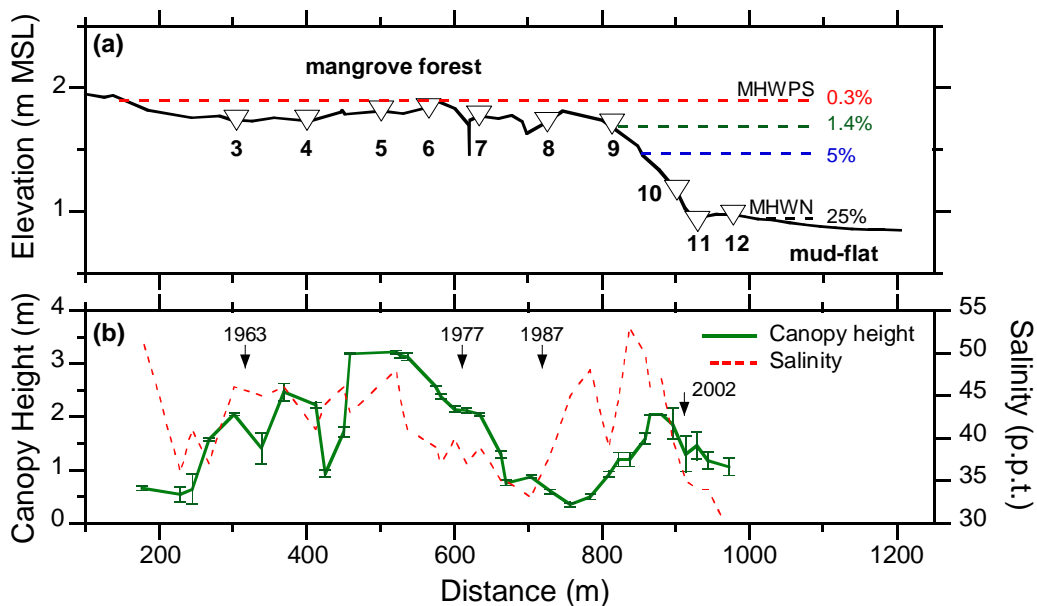


**Fig. 2.** Transect B: (a) bed elevation, tidal inundation (% of total time) and core locations (3–12); (b) average canopy height (std err = 0.01 – 0.03 m) and sediment pore-water salinity (parts per thousand). The positions of historical mangrove seaward fringes are also shown.

The profile is characterized by a uniformly flat surface within the mangrove forest, with elevations of 1.7–1.89 m above MSL and close to the MHWPS tide at 1.87m MSL, apart from a tidal creek (1.49-m MSL). The elevation maximum occurs near LC-6, which coincides with the tallest trees in the forest. This cross-shore sequence is repeated for the present mangrove SEV at 850–950 m. The prograding beach face (LC-9 to LC-11) slopes seaward at  $0.37^\circ$  and is ten-times steeper than the adjacent mudflat. Mean high water neap tide (MHWN, 0.98m MSL) coincides with the mangrove SEV, so that the present fringe on the beach face is only inundated during fortnightly spring tides (Fig. 2a). Predicted MHWS-tide elevation is 1.60 m above MSL. The length of tidal inundation rapidly decreases with increasing intertidal elevation and reduces from 25% on the mangrove SEV to  $< 1.4\%$  for much of the mangrove-forest above 1.7 m MSL. The landward boundary of the mangrove forest is close to MHWPS, which is inundated  $\leq 0.3\%$  of the time. Comparison with predicted tides indicates that the measured meteorological or storm tides increase the length of time that the mangrove forest (above 1.7 m MSL) is flooded by *c.* 40%, which is equivalent to an additional 30 hrs per year. The largest storm tide during 2004–2006 (18 Sept. 2005) at 2.33 m MSL was 0.6 m higher than predicted.

### **Mangrove-forest structure**

The mangrove-forest that has developed over the last 50 years displays a wide range of structure. Canopy height varies from  $< 0.5\text{m}$  to 3.5 m (Fig. 2b). Tree architecture also varies from open, spreading tree forms, which are indicative of trees that have grown in high-light environments without competition on colonizing edges, to trees with very straight trunks that have grown competing for available light. Variation in forest height did not significantly correlate with distance from the 1952 shoreline or porewater salinity. A repeating pattern of taller trees giving way to short, dwarf trees was evident along the cross-shore transect. For example, the current seaward fringe (850-1000 m seaward of the 1952 shoreline) gives way to a dwarf stand, with average canopy heights  $< 0.5\text{ m}$ , between 650–800 m. Landward of these dwarf mangroves, are found the tallest trees (450–600 m), with an average-canopy height of 3 m, where a well developed and clearly older forest occurs. Lichen accumulation on the bark of trees in this tall forest is substantial. The tallest stand gives way to shorter forest again at 560 m, after which forest height increases before declining to be replaced by saltmarsh dominated by glasswort (*Sarcocornia quinqueflora*).

### **Sediment properties**

Sediments deposited since the early-1950's on the mangrove flat (LC-3 to LC-9) are composed of homogenous muds, with median ( $D_{50}$ ) and mean particle diameters  $\leq 20\ \mu\text{m}$  (Figs. 3a–c). Vertical profiles to 1.9-m depth show little variation except near the base of cores LC-8 and LC-9, which show abrupt increases in particle size at about 0.1–0.2 m above MSL. Sediment wet and dry bulk densities are between  $1\text{--}2.4\ \text{g cm}^{-3}$  and  $0.4\text{--}0.8\ \text{g cm}^{-3}$  respectively. Cores LC-10 and LC-11 collected on the mangrove fringe near the base of the actively prograding beach (0.9–1.2 m MSL) sample older deposits down to 0.8 m below MSL. The upper 0.8–1 m of these cores is also composed of homogenous fine-grained mud ( $D_{50} \text{ c. } 15\ \mu\text{m}$ ), below which an abrupt increase in particle size occurs ( $D_{50} > 40\ \mu\text{m}$ ) at 0.17 m above MSL (Figs. 3d–e).

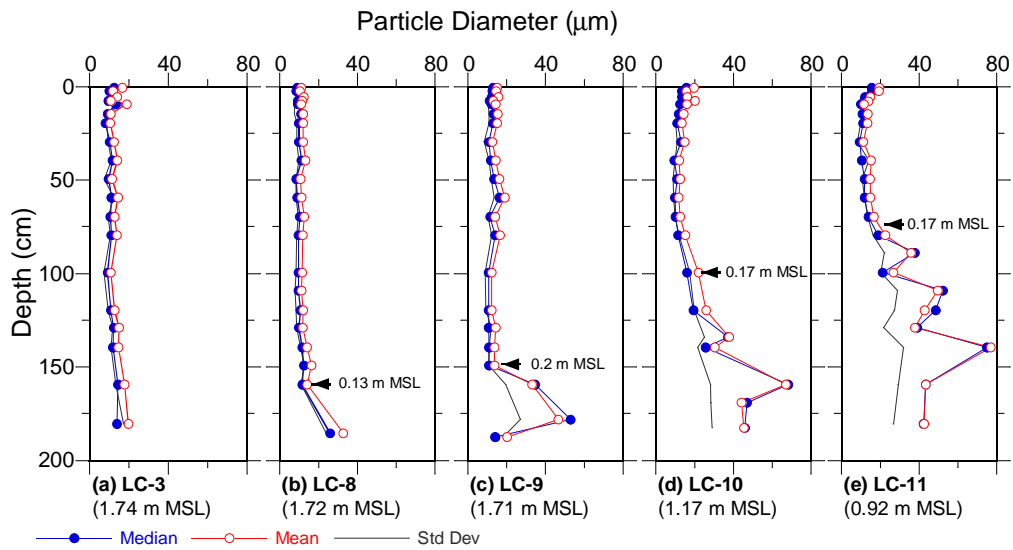


**Fig. 3.** Particle-size profiles for selected cores from the mangrove-forest (LC-3 to -9), seaward fringe (LC-10) and adjacent mudflat (LC-11). Surface elevation at sites is also shown.

Below this *c.* 1-m-thick mud layer, x-radiographs clearly show laminated clays, silts and fine sands overlaying abundant shell valves and hash of cockle (*Chione stuchburyi*) and estuarine trough shell (*Mactra ovata*), which is a suspension feeder characteristic of estuarine intertidal flats. The thickness of the laminations increase in scale with depth from mm to cm. X-radiographs of the T cores (Fig. 4), collected on the open mudflats, are characterized by two distinct zones of contrasting sedimentary fabric.

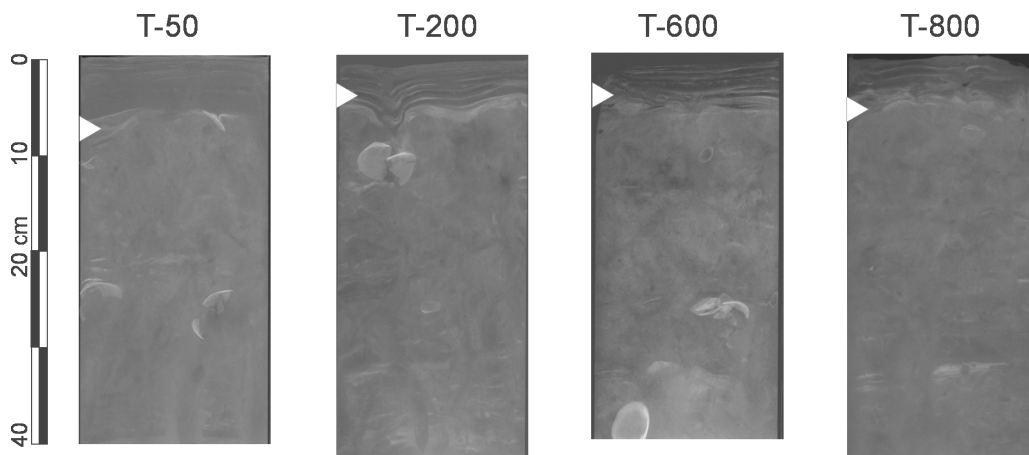


**Fig. 4.** X-radiograph negatives of the T-series cores from the mudflats. Bright shades indicated high-density or coarser sediment, and dark shades indicate low density or finer sediment.  $^7\text{Be}$  penetration depth indicated by white triangles. Shell valves are of *M. ovata*.

A surficial layer, 3-7 cm thick, contains prominent laminations and cm-scale beds that display sharp basal contacts, and grade upward from coarser (light gray in X-radiographs) to finer (darker gray) sediments. These sediments have relatively high water content, as indicated by the dark shades in X-radiographs, and are mostly unbioturbated. Below this stratified surface layer, sediments display a range of biogenic

structures, including indistinct mottling and clearly defined burrows (mostly of polychaetes and *M. ovata*). These biogenic structures have overprinted mm-to-cm-scale stratification that is similar to the surface layer, but less clearly preserved, due to post-depositional bioturbation. Grain-size distributions in open-mudflat cores are slightly coarser than those observed in surface sediments of mangrove cores, with mean particle sizes of 25-43  $\mu\text{m}$ , including 0-13% sand (concentrated in coarser beds evident in Fig. 4).

### Radioisotope distributions

All profiles of  $^{210}\text{Pb}$  in cores display prominent changes in gradients that indicate changes in SAR over time (Fig. 5). The lowermost section of all cores is characterized by a clearly defined region of relatively low SAR (8-25  $\text{mm yr}^{-1}$ ). The upper boundary of this region ranges from 1.5 to 1.7 m below the sediment surface close to the landward margin, to  $\sim 0.25$  m below the sediment surface on the open mudflats at LC-12. Above this basal zone, in cores LC-3 to LC-12, SAR increase (to 33-108  $\text{mm yr}^{-1}$ ). These sub-vertical gradients extend to the sediment surface in cores LC6 to LC-11 (with a prominent discontinuity in LC-6). The surface of core LC-3 is characterized by a less vertical gradient and SAR of 8  $\text{mm yr}^{-1}$  from 0.25 m below the sediment surface to the core top. In contrast, the two seaward-most cores (LC-11 and LC-12) have approximately vertical  $^{210}\text{Pb}$  profiles in the upper  $\sim 0.25\text{m}$  of core, suggesting either: extremely high deposition rates, rapid vertical mixing, or a combination of the two.

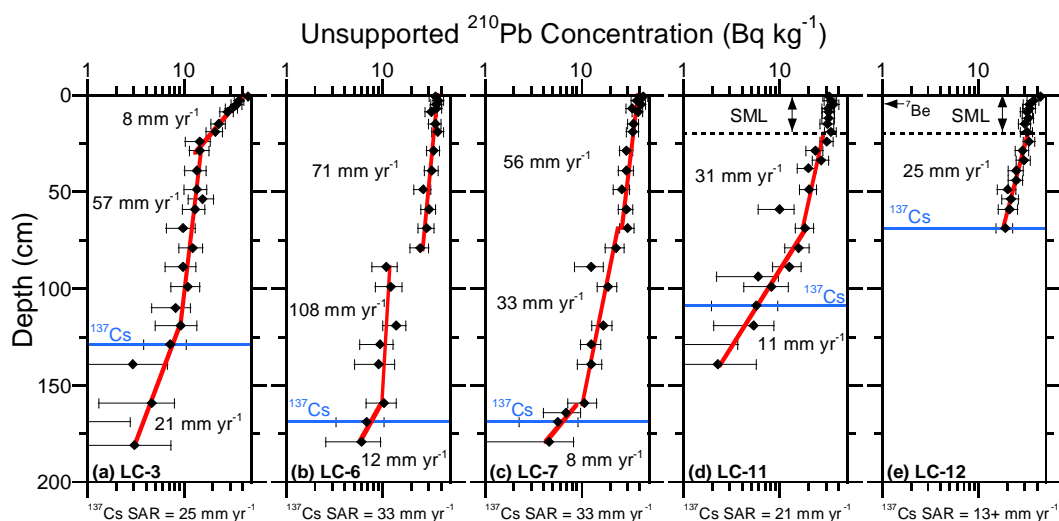


**Fig. 5.**  $^{210}\text{Pb}_{\text{ex}}$  concentration profiles and 95% conf. intervals and SAR for long-core sites (LC): mangrove forest (LC-3–LC-7); mangrove seaward fringe (LC-11); and mudflat (LC-12), Maximum  $^{137}\text{Cs}$  depth and SAR also shown. SML = surface-mixed layer.

The presence of  $^{137}\text{Cs}$  to 169-cm depth in LC-6 and LC-7 shows that these sediments have been deposited since the early 1950s and  $^{137}\text{Cs}$ -derived SAR for the mangrove forest were 21–36  $\text{mm yr}^{-1}$ .  $^7\text{Be}$  occurs to 2-cm depth in cores LC-5 to LC-11 (mangrove forest) and to 4-cm depth in LC-12 (mudflat). Maximum SAR coincide with LC-8 and LC-9 located landward of the present-day mangrove fringe. The  $^{210}\text{Pb}_{\text{ex}}$  inventories (*A*) and mean annual supply rates (*P*) calculated for the long-cores display distinct spatial

patterns (Table 1). Inventories for cores LC-3 to LC-5 taken from the oldest (i.e., pre-1970s) mangrove forest gradually increase seaward.

**Table 1.**  $^{210}\text{Pb}_{\text{ex}}$  inventories (*A*) and mean annual supply rates (*P*) and concentration factors (*C*) in the long cores.

Core	<i>A</i> ( $\text{Bq cm}^{-2}$ )	<i>P</i> ( $\text{Bq cm}^{-2} \text{yr}^{-1}$ )	<i>C</i>
LC-3	1.27	0.039	6.7
LC-4	1.40	0.044	7.4
LC-5	1.59	0.050	8.4
LC-6	3.75	0.117	19.8
LC-7	1.87	0.058	9.9
LC-8	1.73	0.054	9.1
LC-9	1.75	0.055	9.3
LC-10	1.21	0.038	6.4
LC-11	0.15	0.005	0.8

By comparison, *A* is similar for cores taken from mangrove forest established since the late-1970's (LC-7 to LC-9). At LC-6, *A* is more than double that measured at any other site. The concentration factor (*C*) indicates how *P* scales with the measured  $^{210}\text{Pb}$  atmospheric flux ( $0.006 \text{ Bq cm}^{-2} \text{ yr}^{-1}$ ). Table 1 shows that sediments in the mangrove forest are accumulating  $^{210}\text{Pb}_{\text{ex}}$  at rates 6–20 times higher than expected if supplied by direct atmospheric deposition alone (i.e.,  $C = 1$ ).

### Propagule and seedling establishment

Mangrove propagules settled on the mudflat in January 2006 over a 250-m wide band seaward of the present mangrove fringe. Propagule and seedling density at the first survey (28 January 2006) reached up to  $187 \text{ m}^{-2}$ , with a mean density of  $36.4 \pm 3.6 \text{ m}^{-2}$  ( $\pm$  std error,  $n = 90$ ). Propagule and seedling numbers declined rapidly and exponentially over time ( $r^2 = 0.99$ ) so that  $< 10\%$  of the initial propagules remained after 60 days and only one seedling remained after 180 days. Propagule attrition was not significantly influenced by site or distance from the mangrove fringe ( $P > 0.05$ ). Despite the high-attrition rate of propagules, surviving seedlings were actively growing as shown by the proportion of seedlings that entered the 2–3 leaf pair stage after day 23 (Fig. 6).

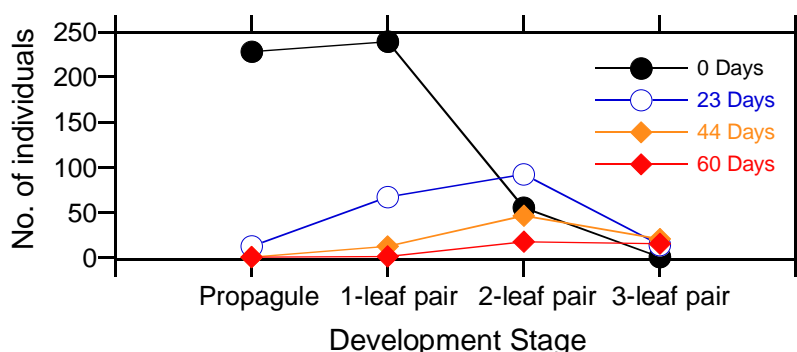


**Fig. 6.** Number of mangrove propagules and seedling in each development stage during the first 60 days of the monitoring.

## DISCUSSION

The recent geomorphic evolution of the Firth is closely linked to historical increases in sediment loads following large-scale catchment deforestation and river-engineering works (1850s–1920s). The estimated  $44 \times 10^6 \text{ m}^3$  of mud was deposited in the southern Firth over a 36-year period to 1918 is equivalent to *c.* 280 years of present-day sediment loads. Cores record the physical effects of this mud influx on the Firth. Below the base of the 0.8–1.6-m thick homogenous mud layer at 0.2-m MSL are the original laminated silts and sands that are characteristic of energetic mixed-sediment intertidal-flats (Reineck and Singh, 1980). The abrupt transition to a pure-mud substrate indicates a fundamental change in the sediments and geomorphology of the Firth, which has initiated a sequence of large-scale environmental change. These changes include the rapid mangrove-habitat expansion that began in the 1950's, which continues today. Similar environmental changes have occurred in many N.Z. estuaries. However, the magnitude of these changes has been much larger in the Firth.

$^{210}\text{Pb}_{\text{ex}}$  profiles record the temporal and spatial sequence of initial mangrove colonization and mangrove-habitat expansion over the last 50 years.  $^{210}\text{Pb}_{\text{ex}}$  profiles in cores from the oldest mangrove stand (LC-3 to LC-5) closest to the 1952 shoreline show a characteristic stair-step form (Fig. 5a), which are consistent with the known chronology of mangrove colonization and  $^{137}\text{Cs}$  dating. Core LC-3 provides the longest record of sedimentation dating back to the 1920s (Fig. 5a) with SAR averaging  $20 \text{ mm yr}^{-1}$  that are similar to the present-day mudflat ( $25 \text{ mm yr}^{-1}$ , Fig. 5e). These values are 5–10 times higher than SAR observed in other North-Island estuaries. Mangrove colonization resulted in a three-fold increase in SAR, with one metre of sediment deposited at LC-3 in little more than a decade. As the mangrove-forest expanded seawards so did the locus of maximum SAR. This process is recorded in cores from the oldest mangrove stand by an abrupt reduction in SAR to  $8\text{--}11 \text{ mm yr}^{-1}$  from the late 1960s onwards (Fig. 5a), as the sediment supply from open mudflats was cut off by forest expansion. Core LC-6 displays a discontinuity at 80–85-cm depth (Fig. 5b), with substantially lower  $^{210}\text{Pb}_{\text{ex}}$  concentrations below this layer than above and SAR of  $71\text{--}108 \text{ mm yr}^{-1}$ . Cores LC-7 (Fig. 5c) to LC-9 also show that the mudflat was rapidly accumulating ( $21\text{--}33 \text{ mm yr}^{-1}$ ) even before mangroves colonised these sites (late 1970s–) and further increasing SAR ( $53\text{--}56 \text{ mm yr}^{-1}$ ). The present-day mangrove SEV established in last decade is also rapidly accumulating sediment (LC-11, Fig. 5d). X-radiographs and  $^7\text{Be}$  profiles ( $\leq 7\text{-cm}$ ) from the mudflat (Fig. 4) show that sediment resuspension and/or deposition introduces  $^7\text{Be}$  into the seabed, rather than bioturbation.  $^{210}\text{Pb}_{\text{ex}}$  inventories in the cores indicate that the mangrove-forest is a major long-term sink for fine sediments.

In many mangrove ecosystems canopy height reduces with distance from the seaward fringe. This reflects a reduction in tidal-water, nutrient and sediment inputs and an increase in salinity as evaporation exceeds tidal recharge (Smith, 1992). In the Firth, the complex variation in forest structure suggests multiple forest building events (Fig. 2b). This system provides an important case study of how mangrove forests develop through time, and a baseline to investigate how the function of mangrove ecosystems change as they undergo succession. Mortality of propagules and seedlings on the mudflat is primarily due to episodic wave-driven erosion of the substrate in which the seedlings are

rooted. In southern Australian, wind and wave conditions are also the most important factors influencing *A.marina* seedling mortality in estuaries (Clarke and Myerscough 1991). The early development of seedlings (Fig. 6) indicates that conditions are suitable for growth in the absence of physical disturbance. The repeating pattern of tall seaward-fringing forest and short/dwarf forest landward and observed high seedling mortality on the mudflats suggests that major phases of mangrove-habitat expansion have occurred infrequently and likely coincide with extended periods of unusually calm weather conditions that are required for successful seedling establishment

Mangrove colonization of the upper-intertidal flat at LC-3 occurred when the bed elevation was  $\geq 0.5$  m above MSL (Fig. 5a). This is well above the 0-m MSL lower-elevation limit (LEL) for grey mangrove (Clarke and Myerscough, 1993). The intertidal flat was rapidly accreting mud and by the 1950s eventually reached a critical elevation, with mangrove colonising the site during a period of calm weather. In nearby Tauranga Harbour, with its smaller wave fetch, the LEL for mangrove at wave-exposed sites is *c.* 0.3 m above MSL. Tidal range also influences the LEL for mangrove because wave-energy expended across the intertidal flats varies with water depth due to water-column attenuation and bed-friction effects for the short-period waves typical of New Zealand's fetch-limited shallow estuaries (Green et al., 1997; Swales et al., 2004). We normalised LEL for mangrove for both estuaries by the "king tide" amplitude to obtain a non-dimensional LEL of 0.3 for both estuaries. This approach could potentially be useful for predicting future mangrove colonization and habitat expansion in estuaries.

The fate of mangrove-forests primarily depends on the surface elevation increasing at a rate equal to or exceeding sea level rise (SLR). This has previously been assessed by comparing SAR derived from cores with SLR but is complicated by the effects of sediment auto-compaction (Cahoon et al., 1999). Furthermore, the frequency and duration of flooding by tides and freshwater runoff varies with elevation and controls sediment delivery, substrate oxidation and plant growth. Sedimentation-Erosion Tables (SET) have been used to apportion substrate elevation changes due to shallow subsidence and sedimentation. Cahoon et al. (1999) reported that: (1) surface-elevation gains lagged SAR at 50% of the 43 SET sites studied; and (2) surface-elevation change is a more suitable predictor of the future effects of SLR on mangrove/marsh stability. In the Firth, SAR of 8–100 mm yr<sup>-1</sup> have substantially out paced SLR (1.3 mm yr<sup>-1</sup>) so that the mangrove forest is now close to the upper limit of the tide and is very infrequently flooded. Surface elevations within the forest vary by < 20-cm despite large spatial variations in SAR. This suggests a complex feedback between the physical and biological processes controlling substrate elevation that has not yet been determined.

## CONCLUSION

Rapid mangrove-habitat expansion in the Firth of Thames over the last 50 years is closely linked to historical increases in sediment loads due to catchment deforestation since the mid-1800s. The large quantities of mud deposited in the Firth over the next several decades buried the original laminated silt–sand substrate. Dated cores indicate that the upper-intertidal flats were rapidly accreting mud (20 mm yr<sup>-1</sup>) for several decades. This initiated a sequence of large-scale environmental change that included

rapid mangrove colonization and habitat expansion since the 1950s. Mangrove-habitat expansion further increased SAR ( $\leq 100 \text{ mm yr}^{-1}$ ), rapidly building and elevating vegetated mudflats. The mangrove forest is a major long-term sink for fine sediments. Seedling recruitment is largely controlled by wave-driven erosion of the mudflat to  $\leq 7$ -cm depth. Major periods of mangrove-forest expansion have been infrequent and have likely coincided with extended periods of calm weather. The lower-elevation limit for mangrove colonization at *c.* 0.5 m above MSL was higher than expected due to wave exposure. The mangrove forest is now near the upper limit of the tides and is infrequently flooded. Most sediment is deposited along the seaward fringe of the forest so that sedimentation decreases landward ( $50$  to  $8 \text{ mm yr}^{-1}$ ) due to reduced sediment supply and accommodation space. The long-term fate of this mangrove system depends on the surface elevation increasing at a rate equal to or exceeding SLR. This cannot be evaluated from sediment cores alone, due to the complications arising from shallow subsidence and the feedbacks between physical and biological processes.

### ACKNOWLEDGEMENTS

Dr Terry Hume (NIWA) reviewed the paper and Mr Ron Ovenden (NIWA) undertook the elevation surveys and processed the sediment cores. Radioisotope analyses (LC cores) were conducted by the N.Z. National Radiation Laboratory. Dr Brian Sorrell (NIWA) participated in the ecological study. We thank Mr Rick Liefing (Environment Waikato) for supporting the initiation of this study. The study was funded by the NZ Foundation for Research Science and Technology (CO1X0307) and Environment Waikato. Funding to S. Bentley was provided through a NIWA visiting-scientist fellowship, and the US National Science Foundation (CAREER grant OCE-0093204).

### REFERENCES

- Augustinus, P.G.E.F. (1980). "Actual development of the chenier coast of Suriname (South America)," *Sedimentary Geology* 26, 91–113.
- Burns, B.R. and Ogden, J. (1985). "The demography of the temperate mangrove (*Avicennia marina* (Forsk.) Vierh.) at its southern limit in New Zealand," *Australian Journal of Ecology* 10, 125-133.
- Brownell, B. (2004). "Muddy feet: Firth of Thames RAMSAR-site update 2004," Ecoquest Education Foundation, Pokeno, New Zealand, 198 p.
- Cahoon, D., Day, J.W., Reed, D.J. (1999). "The influence of surface and shallow subsurface soil processes on wetland elevation: a synthesis," *Current topics in wetland biogeochemistry* 3, 72–88.
- Cintrón, G. and Schaffer-Novelli, Y. (1984). "Methods for studying mangrove structures," p 91-113. *In*: S.C. Saenger, and J.G. Snedaker (eds.). The mangrove ecosystem: research methods. *UNESCO Monographs in Oceanographic Methodology* 8.
- Clarke, P.J. and Myerscough, P.J. (1993). "The intertidal distribution of the grey mangrove (*Avicennia marina*) in southeastern Australia: The effects of physical conditions, interspecific competition, and predation on propagule establishment and survival," *Australian Journal of Ecology* 18, 307–315.
- Ellis, J, Nicholls, P., Craggs, R., Hofstra, D. and Hewitt, J. (2004). "Effects of terrigenous sedimentation on mangrove physiology and associated macrobenthic

- communities,” *Marine Ecology Progress Series* 270, 71-82.
- Mehta, A. J. (2002). “Mud-shore dynamics and controls,” p 19–60. *In: Healy, T., Yang, J.-A. Healy, (eds.) Muddy coasts of the world: processes, deposits and function.*
- Neil, D.T. (1998). “Moreton Bay and its catchment: seascape and landscape, development and degradation,” *In Tibbetts IR, Hall NJ, Dennison WC (eds.), Moreton Bay and Catchment, University of Queensland, p. 3–54.*
- Furukawa, K., Wolanski, E. and Mueller, H. (1997). “Currents and sediment transport in mangrove forests,” *Estuarine, Coastal and Shelf Science* 44, 301–310.
- Green, M.O., Black, K.P., and Amos, C. L. (1997). “Control of estuarine sediment dynamics by interactions between currents and waves at several scales,” *Marine Geology* 144, 97–116.
- Healy, T. (2002). “Muddy coasts of mid-latitude oceanic islands on an active plate margin – New Zealand,” p 347–374. *In: Healy, T., Yang, J.-A. Healy, (eds.) Muddy coasts of the world: processes, deposits and function.*
- Hume, T.M. and McGlone, M.S. (1986). “Sedimentation patterns and catchment use changes recorded in the sediments of a shallow tidal creek, Lucas Creek, Upper Waitemata Harbour, New Zealand,” *N.Z. Journal of Marine and Freshwater Research*, 20, 677–687.
- Milliman, J.D. and Syvitski, J.P.M. (1992). “Geomorphic/Tectonic control of sediment discharge to the ocean: The importance of small mountainous rivers,” *Journal of Geology* 100, 525–544.
- McKee, K. L., Mendelssohn, I.A. and Hester, M.W. (1988). “Re-examination of pore water sulfide concentrations and redox potentials near the aerial roots of *Rhizophora mangle* and *Avicennia germinans*,” *American Journal of Botany* 75, 52–1359.
- Reineck, H.E. and Singh, I.B. (1980). “Depositional Sedimentary Environments, second revised edition,” Springer-Verlag, Berlin.
- Smith, T. J., III. (1992). “Forest structure,” *In Robertson, A.I., and Alongi, D.M. (eds.), Tropical Mangrove Ecosystems, Coastal and Estuarine Studies, 41. American Geophysical Union. Washington DC. pp. 101-136.*
- Swales, A., Williamson, R.B., Van Dam, L.F. and Stroud, M.J. (2002). “Reconstruction of urban stormwater contamination of an estuary using catchment history and sediment profile dating,” *Estuaries* 25(1), 43–56.
- Swales, A., MacDonald, I.T. and Green, M.O. (2004). “Influence of wave and sediment dynamics on Cordgrass (*Spartina anglica*) growth and sediment accumulation on an exposed intertidal flat,” *Estuaries* 27(2), 225–243.
- Thom, B.G., Wright, L.D., Coleman, J.M. (1975). “Mangrove ecology and deltaic geomorphology: Cambridge–Ord River, Western Australia,” *J. Ecology* 63, 203–232.
- Thrush, S.F., Hewitt, J.E., Cummings, V.J., Ellis, J.I., Hatton, C., Lohrer, A., Norkko, A. (2004). “Muddy waters: elevating sediment input to coastal and estuarine habitats,” *Frontiers in Ecology and Evolution* 2, 299-306.
- Wells, J.T. and Coleman, J.M. (1981). “Physical processes and fine-grained sediment dynamics, coast of Surinam, South America,” *Journal of Sedimentary Petrology* 51, 1053–1068.
- Woodroffe, C.D., Curtis, R.J., McLean, R.F. (1983). “Development of a chenier plain, Firth of Thames, New Zealand,” *Marine Geology* 53, 1–22.